REPORT DOCUMENTATION PAGE

AFRL-SR-AR-TR-03-

0334

PLEASE DO NOT RETURN YOUR FORM TO THE ABOVE ADDRESS.

1. REPORT DATE (DD-MM-YYYY)	2. REPORT TYPE	3. DATES COVERED (From - To)
21-07-2003	FINAL	21 May 2003 - 30 April 2003

4. TITLE AND SUBTITLE

DURIP-FY2002: Instrumentation for the Comprehensive Optical Analysis of Luminescence Sensors

5a. CONTRACT NUMBER

F49620-02-1-0199

5b. GRANT NUMBER

5c. PROGRAM ELEMENT NUMBER

6. AUTHOR(S)

Daniel G. Nocera

5d. PROJECT NUMBER

5e. TASK NUMBER

5f. WORK UNIT NUMBER

7. PERFORMING ORGANIZATION NAME(S) AND ADDRESS(ES)

Massachusetts Institute of Technology
Department of Chemistry, 6-335
77 Massachusetts Avenue
Cambridge MA 02139

8. PERFORMING ORGANIZATION REPORT NUMBER

9. SPONSORING/MONITORING AGENCY NAME(S) AND ADDRESS(ES)

USAF, AFRL
AF Office of Scientific Research
801 N. Randolph Street, Room 732
Arlington MA 22203
Pat Bell 703 696 9730 (patricia.bell@afosr.af.mil)

10. SPONSOR/MONITOR'S ACRONYM(S)

AFOSR/PK2

11. SPONSOR/MONITOR'S REPORT NUMBER(S)

12. DISTRIBUTION/AVAILABILITY STATEMENT

Unlimited.

13. SUPPLEMENTARY NOTES

20030915 016

14. ABSTRACT

This proposal requested DURIP funding for the assembly of a spectroscopic facility for the comprehensive optical analysis of luminescence sensors (COALS). The COALS system is comprised of three components: absorption, emission and infrared spectrophotometers. The instrumentation provides research students of project F49620-01-1-0118 (Optical Supramolecules for Chemical and Physical Sensing, PI - Daniel G. Nocera) a powerful set of tools for their characterization of newly created luminescent molecules, supramolecules and materials. These new light-emitting substances form the underpinning to the novel sensing methods and techniques invented under the auspices of F49620-01-1-0118. The spectroscopic instrumentation was augmented with a computer cluster, designed to perform high level ab initio and density functional calculations. These calculations have been invaluable in assisting students in their interpretation of data collected from the COALS system.

15. SUBJECT TERMS

luminescence, emission, absorption, infrared, computational cluster, density functional theory, supramolecule, chemosensor, molecular tagging velocimetry, quantum dot, nanocrystal, pressure sensitive paint, microfluidics

16. SECURITY CLASSIFICATION OF:			17. LIMITATION OF ABSTRACT	18. NUMBER OF PAGES	19a. NAME OF RESPONSIBLE PERSON
a. REPORT	b. ABSTRACT	c. THIS PAGE			19b. TELEPHONE NUMBER (Include area code)
U	U	U	UU	12	

1. Introduction

DURIP funding was used to assemble a spectroscopic facility for the comprehensive optical analysis of luminescence sensors (COALS). The COALS system is comprised of three components: absorption (steady-state and time-resolved), emission (steady-state and time-resolved) and infrared (time-resolved) spectrophotometers. The spectroscopic instrumentation was augmented with a computer cluster, designed to perform high level *ab initio* and density functional calculations. These calculations have been invaluable in assisting students in their interpretation of data collected from the COALS system. An itemized list of the purchased equipment follows.

Emission/Absorption	
Diode array/UV computer	2,111.20
Arc lamp, reflector, mercury lamp	14,238.00
Fluorometer	44,962.00
Photomultiplier tubes	2,142.56
Dual syringe	3,206.44
Printer	1,489.52
Computer	1,055.60
DCIF HE transfer line	5,467.74
Infrared OPA	
Jade laser	37,075.91
Stage/base/poles	381.80
Lens/stages	1,128.62
Mirror/stage	2,294.28
Waveplate/mirror	859.39
Reflectors	594.00
Grating	3,993.91
Computational cluster	
Computers	28,180.00
Cabinet	2,442.55
Total	$151,622.72

The instrumentation provides research students of project F49620-01-1-0118 (*Optical Supramolecules for Chemical and Physical Sensing*, PI - Daniel G. Nocera) a powerful set of tools for their characterization of newly created luminescent molecules, supramolecules and materials. These new light-emitting substances form the underpinning to the novel sensing methods and techniques invented under the auspices of F49620-01-1-0118. Three projects, addressing the diverse chemical and physical sensing needs of the United States Air Force have benefited from the DURIP instrumentation: (1) Supramolecular MicroFluidic Optical Chemosensors for the nanoscopic detection and monitoring of chemical and biomolecule species of relevance to the Air; (2) Tracers for Molecular Tagging Velocimetry to quantitatively measure the structure of highly turbulent flows of importance to the Air Force; and (3) New Pressure Sensitive Paint Tracers to sense and measure pressure over aerodynamic surfaces under

investigation at AFOSR testing facilities. All newly discovered sensing methods and techniques of projects (1) - (3) are based on monitoring a bright luminescence. The DURIP instrumentation allows us to define the most fundamental suite of photophysical properties: the absorption, emission and vibrational properties of newly created lumophores. With this information in hand, pathways that circumvent efficient light emission can be identified and designed out of the lumophore, thus enabling us to produce optimized systems to meet Air Force sensing needs.

From an educational perspective, the COALS system has provided a training ground for this century's cohort of scientific professionals that apply spectroscopy in unique ways to solve important problems for the DOD. Students at the graduate level are applying the DURIP instrumentation to a broad scope of problems spanning chemistry and engineering. The near-term payoff to the DOD is the science that these students discover. A longer-term payoff will be the continued involvement of these students in Air Force research programs after graduation. Indeed, recent students of F49620-01-1-0118 have accepted permanent positions at DOD labs to continue their work for the AFOSR.

The requested DURIP instrumentation had strong cost sharing and infrastructure support. MIT allocated over 1,500 square feet (at $\$500/ft^2$) of new laboratory space for the proposed instrumentation. The Institute underwrote the costs for the renovation of this space.

A technical summary of the science in projects (1) - (3) that utilized the COALS instrumentation is now presented.

2. 3R Chemosensing

A benchmark of this program is the development of "3R" – recognize, relay, report – chemosensing. A major goal of the previous funding cycle was to implement 3R chemosensing on microfluidic length scales. In this section, new advances in the fundamental science and application of 3R chemosensing will be described. The section concludes with a summary of our design of the first microfluidic optical chemosensor.

2.1. Mechanistic Studies

The basic 3R approach is schematically outlined in Figure 1 [*3.1.4.1*]. A non-covalent molecular recognition event at the receptor site is communicated, by physical or chemical means, to a reporter site, which produces a measurable signal. A rapid equilibrium between the analyte and the receptor site affords the chemosensor a real-time response that varies with analyte concentration. We have applied the 3R approach to detect chemical signatures of jet fuels for field monitoring and environmental remediation at United States Air Force bases and storage facilities. The evolutionary members of the chemosensors designed for this application are shown in Figure 2. In our design, a cyclodextrin (CD) was used as the recognition site, a terbium ion (Tb^{3+}) was the reporting site, which was excited by an energy transfer relay from the mono- or bicyclic

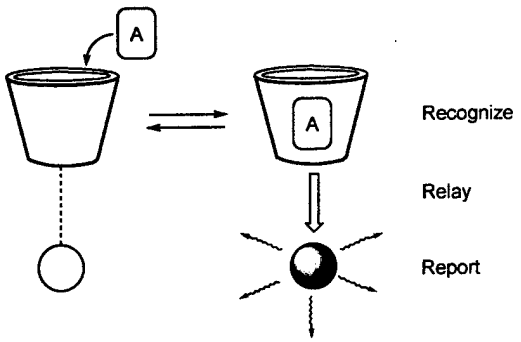

Figure 1. *The 3R scheme used for chemosensor development. A = analyte.*

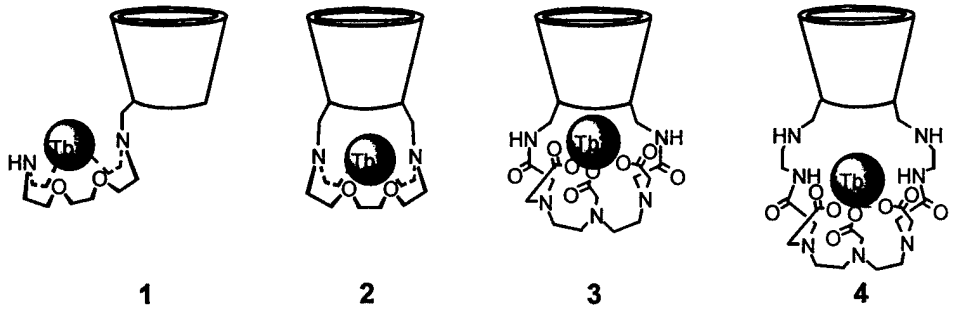

Figure 2. *Different chemosensors designed for the detection of PAHs by the 3R approach.*

polyaromatic hydrocarbon (PAH). β-CD (7 D-glucose rings composing the bucket) binds BTEXs (benzene, toluene, ethylbenzene, xylene) and bicyclic aromatics (e.g., naphthalene, biphenyl) but not larger polyaromatics. Because we were interested in total aromatic content for the Air Force, β-CD proved to be the ideal receptor site for our targeted chemosensing application.

An important design element of the chemosensors in Figure 2 is that the luminescent signal is triggered upon recognition of analyte by the CD. Thus the presence of PAH is detected by a visible signal against a dark background. Of the chemosensors shown in Figure 2, **3** possesses the most ideal properties for eliciting a triggered signal upon PAH recognition for the reasons presented in our recent review of the subject [*3.1.4.1*]. Because **1-3** pre-date the DURIP funding period, these molecules will not be discussed further. However **4** represents a new chemosensor developed during the DURIP funding cycle that was developed to contribute critically to our understanding of the relay mechanism [*3.1.4.2*].

Chemosensor **4** was prepared by the method outlined in Scheme 1. The methodology permits the distance between the Tb^{3+} reporter site and CD binding site to be increased with respect to **3** while maintaining the same regiochemistry. Despite comparable binding of PAHs to **3** and **4** and identical coordination spheres (neither has water coordinated to the Tb^{3+} ion as established by Horrock's photophysical method), the latter produces a triggered signal with a dramatically reduced intensity (by a factor of 16) for model PAHs such as biphenyl. Moreover,

Scheme 1

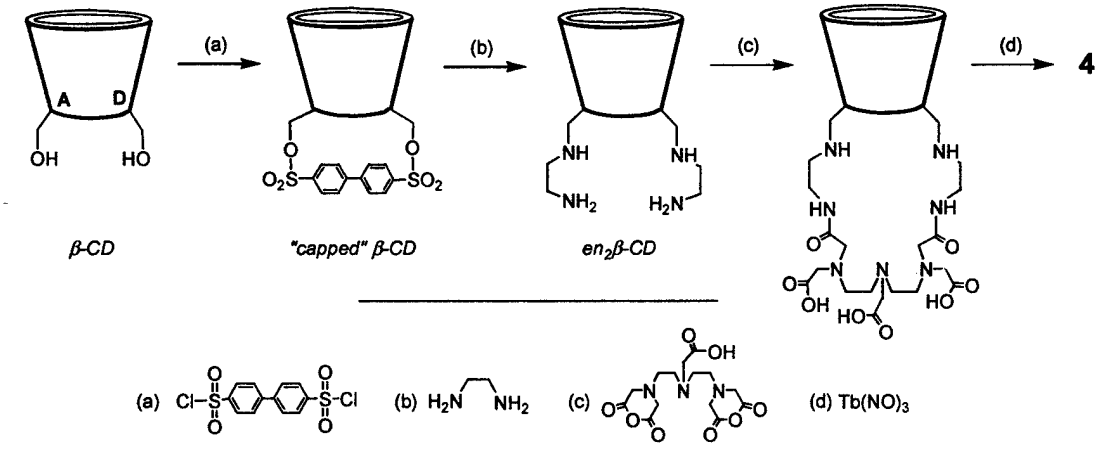

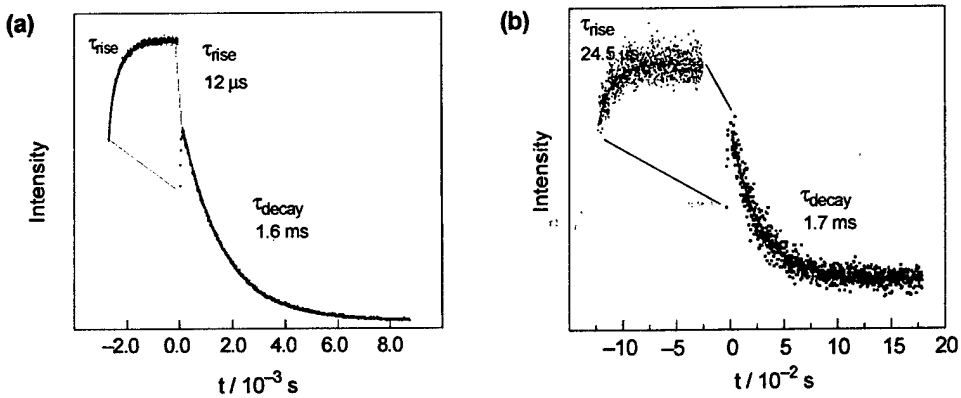

Figure 3. *The growth and subsequent decay of Tb^{3+} luminescence (λ_{em} = 546 nm) from (a) **3** and (b) **4** upon the excitation of biphenyl with the fourth harmonic of a Nd:YAG nanosecond laser (λ_{exc} = 273 nm). The exponential fits of the data, from which the risetime and decay rate constants were derived, are displayed by the solid lines.*

time-resolved measurements (Figure 3) show that the appearance of Tb^{3+} emission from **4** appears on a timescale that is twice as slow as that observed from **3**; both exhibit the natural decay lifetime of 1.6 ms for the Tb^{3+} ion. A thorough analysis of these data establishes that the energy transfer mechanism is Dexter and not Förster (due to the low absorption cross-section of the $^7F_J \rightarrow {}^5D_4$ transition of the Tb^{3+} ion). A Dexter treatment of these time-resolved energy transfer kinetics predicts the donor-acceptor distance in **4** to increase by 1.8 Å, a distance that is concordant with the distance measurements from energy minimized molecular modeling calculations. Moreover, simple bond length calculations for the added ethylenediamine (en) spacer place the binding site for **4** 1.95 Å further away than that for **3**. The differences in the energy transfer rate constant, k_{en}, between **3** and **4** are thus accounted for by the change in donor-acceptor separation, ΔR_{DA}. However, the energy transfer rates does not solely account for the ×16 difference in luminescence intensity of the two chemosensors. Increasing distance also causes a decrease in spin-orbit coupling interaction,

$$H_{SO} = \sum \frac{Ze^2}{4m^2c^2}\left(\frac{1}{R^3}\right)\ell \cdot s \qquad (1)$$

where Z is the atomic number, m is the mass, ℓ and s are the orbital and spin angular momentum operators, respectively. This is an important contributing factor to chemosensor function because the initially prepared $^1\pi\pi^*$ excited state of the PAH is too short-lived to participate in energy transfer. The Tb^{3+} ion facilitates intersystem crossing to the $^3\pi\pi^*$ whereupon energy transfer occurs to produce the $^5D_4$ emissive excited state of the Tb^{3+} ion. The increase in R_{DA} for **4** is manifested in a smaller yield of $^3\pi\pi^*$ and thus less intense emission upon PAH recognition. This result serves to highlight a little recognized feature in the signal transduction pathways of optical chemosensors, especially those involving Tb^{3+} ions as the light-emitting center. In addition to the obvious importance of the Tb^{3+} ion as the emitting center in the energy transfer process, the Tb^{3+} ion also provides a mechanism to produce a long-lived donor excited state from which energy transfer may occur. In the absence of this heavy atom effect, the singlet-excited state of the aromatic would return to its ground state before energy transfer could occur. By channeling the singlet to a long-lived triplet, ample time is provided for the slower energy transfer process to effectively compete with the fast natural radiative and nonradiative processes of the analyte.

2.2. New Excited States

A fundamental activity of this program is the discovery and elucidation of new excited states. For the purposes of the proposed research effort, we became interested in the developing intense luminescent dyes of exceptional chemical and optical stability. Our attention turned to all inorganic clusters $[Re_6Q_8L_6]^z$ (Q = S, Se; L = σ-donor ligand), which are solely composed of stable metal-metal and metal-chalcogenide bonds. The structures of these clusters, shown in Figure 4, consist of an octahedral metal core coordinated by eight-face bridging X or Q ligands and six axial L donor ligands. They exhibit exceptional thermal stabilities, as they are prepared from high temperature liquid melts (600-800 °C). Upon UV-visible excitation, they emit brilliant red phosphorescence with microsecond length lifetimes. The promise of these clusters as dyes for sensor constructs of Section 3.2.1 provided an impetus for understanding the fundamental factors controlling their excited state properties. We undertook a detailed study of the electronic structure, photophysics and vibrational spectroscopy of 24 $[Re_6S_8]^{2+}$ and $[Re_6Se_8]^{2+}$ with the goal of precisely defining the nonradiative decay mechanism in these clusters [*3.1.4.3, 3.1.4.4*]. The principle findings from this work are as follows.

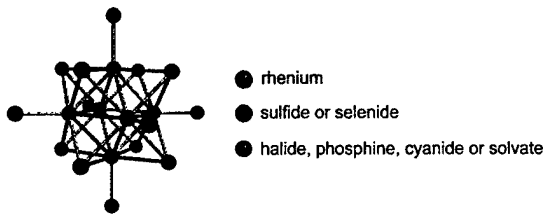

Figure 4. *Structure of $[Re_6Q_8L_6]^z$ (Q = S, Se; L = σ-donor ligand) clusters.*

(a) Room-temperature luminescence lifetimes of the clusters in fluid solution range from 2-22 μs, and quantum yields, from *ca.* 1-22%. Solid-state emission lifetimes and quantum yields occupy a similar range at room temperature.

(b) The long lifetimes, large Stokes shifts and excited-state quenching by O_2 indicate an emitting excited state with considerable spin-triplet character. This was confirmed by electronic structure calculations of the lowest energy excited state.

(c) Those species with oxygen donor ligands deliver maximal quantum yields, the longest lifetimes, and the highest energy emission. Conversely, clusters having six soft, polarizable ligands, such as iodide, emit with less intensity, shorter life spans, and redder luminescence.

(d) $[Re_6S_8]^{2+}$ and $[Re_6Se_8]^{2+}$ emission obeys the approximate energy gap law. This observation implies a common lumophoric kernel in $[Re_6Q_8]^{2+}$ (Q = S, Se) species. It also suggests that these clusters, once excited, share a common deactivation mechanism.

(e) Electronic structure calculations are consistent with energy gap law predictions. Quasi-relativistic electronic structure calculations indicate a lowest energy excited state parentage that is largely localized on the cluster core. These parentages are shown in Figure 5.

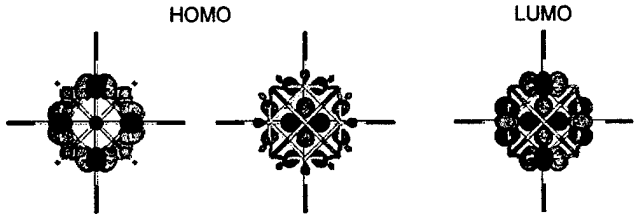

Figure 5. *Degenerate e_g HOMOs and a_{2g} LUMO calculated at the B3LYP/LANL2DZ level of theory.*

(f) Group theory predicts that, for a cluster of ^3E_g excited state parentage in O_h symmetry, deactivating vibrations span the A_{1g} and E_g irreducible representations. A normal mode analysis indicates three A_{1g} and six E_g modes that

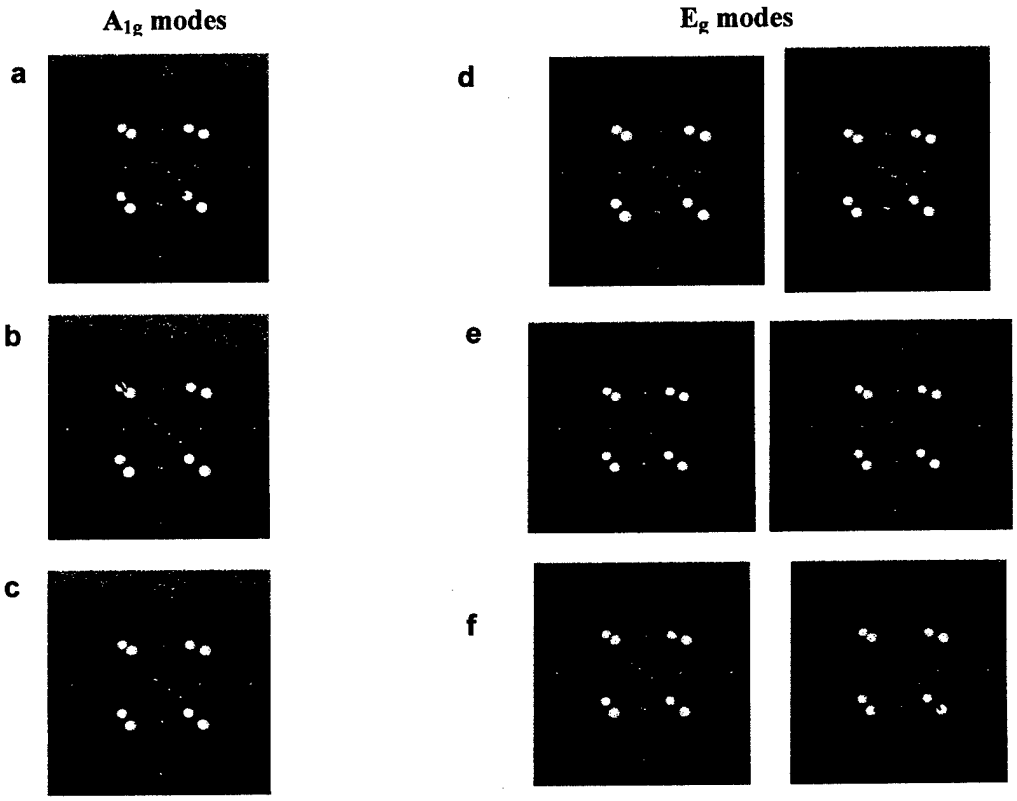

Figure 6. *The (a) $\nu_{a1g}(Re_6)$, (b) $\nu_{a1g}(S_8)$ and (c) $\nu_{a1g}(Cl_6)$ totally symmetric vibrational modes of $[Re_6S_8Cl_6]^{4-}$ and the E_g vibrations of $[Re_6S_8Cl_6]^{4-}$ at (d) 172 cm^{-1} ($\nu_{eg}(obsd)$ = 162 cm^{-1}), (e) 244 cm^{-1}, (calculated intensity is small, bands not observed) and (f) 302 cm^{-1} ($\nu_{eg}(obsd)$ = 277 cm^{-1}). Calculated frequencies were obtained from the HF/enhanced basis level of theory.*

collectively involve the three shells of the cluster structure: the Re_6 octahedron, the S_8 cube of face-bridging chalcogenides, and the six axial ligands. The modes are shown in Figure 6 (g) The calculated modes of (f) are all observed in single crystal Raman spectra in the low-frequency (≤ 100 - 450 cm^{-1}) range. Polarization measurements identify the A_{1g}-symmetric breathing modes; the E_g vibrations were assigned by comparison with quantum chemical/normal coordinate calculations.

(h) Analysis of the emission second central moment provides an effective deactivating vibrational frequency, $\hbar\omega_{eff}$, for individual clusters. The experimental range is ~150 - 350 cm^{-1}. This frequency span coincides with the vibrational energies of the $[Re_6Q_8]^{2+}$ kernel presented in (f), supporting the notion of a core-centered excited state. Substitution of the second-moment derived $\hbar\omega_{eff}$ into the approximate energy gap law reproduces the observed photophysical parameters. This observation affirms the validity of the second moment analysis.

(i) Clusters possessing axial phosphine, cyanide and solvate ligands possess modes of sufficient energy, for energy gap law purposes, to be discernible from other intracluster vibrations. Notwithstanding, these clusters obey the energy gap law correlation, indicating that the emitting excited state is insulated from vibrations of ligands attached to the emitting core at the axial coordination site.

(j) The structural transformation accompanying nonradiative decay of $[Re_6Q_8]^{2+}$ clusters was identified from temperature-dependent photophysical measurements and hybrid density-functional calculations to be tetragonally flattened ($D_{4h}(^3B_{1g})$) → octahedral ($O_h(^1A_{1g})$) singlet ground state. The activation energy for this transformation was experimentally determined to be ~1500-2000 cm^{-1}, which was reproduced from time-dependent DFT calculations. These findings concur with (e) - (i) since it is logical that core localized vibrations will be excited as the $[Re_6Q_8]^{2+}$ clusters dismount from the long-lived excited state to the ground state.

Our work constitutes the most comprehensive single study of metallocluster-based luminescence to date. The combined spectroscopic, computational and photophysical results show that long-lived and bright luminescence may be obtained as long as the $[Re_6Q_8]^{2+}$ core is unperturbed, regardless of the nature of the axial ligand. Thus the axial ligands provide handles for chemical modification of a cluster core that effectively constitutes a molecular light bulb. This result might be exploited in the use of these stable metal-metal bonded species as dyes for the amplification medium of the lasing architectures in future work that will be undertaken in F49620-01-1-0118.

2.3. Micro-Fluidic Optical Chemosensor

MicroFluidic (μF) platforms have emerged as an important technology for chemo- and bioanalytical applications. The miniaturization offered by μF devices allows for the analysis of fluid samples to be performed on a chip, leading to advantages such as reduced sample volume, increased reaction speed and the possibility of massive parallelism. To date, optical analysis on μF platforms has been performed by direct spectroscopic detection methods. The advantages that 3R sensing offers over direct detection methods motivated us to investigate whether 3R function could be transferred to μF platforms. By combining organic and materials synthesis with lithographic patterning methods and undertaking both steady-state and time-resolved spectroscopy on patterned devices, we have shown during the past funding cycle that the complicated signal transduction mechanisms of the supramolecular optical chemosensors may be established in the microdomain. From the knowledge garnered from this effort, we have fabricated the first microFluidic Optical Chemosensor (μFOC).

The realization of μFOCs demanded that a supramolecule architecture be incorporated into a matrix that is compatible with lithographic patterning protocols. Accordingly, a major thrust of our work was to develop methods to permit the attachment of the CD chemosensor onto a substrate. Many syntheses were explored and we were successful in incorporating **3** into organic and inorganic polymer matrices. The most successful films for μFOC detection were prepared according to the method shown in Scheme 2. The CD was condensed into a partially hydrolyzed tetraethylorthosilicate solution in ethanol (acid catalyzed conditions). This solution was spin-cast onto clean, dry, quartz substrate to give gel films of thicknesses ranging from 0.2 - 0.6 μm, as determined by profilometry measurements. Squares of these sol-gel films were photo-lithographically patterned within the serpentine channel of the device shown in Scheme 2. The device exhibits excellent optical response to polyaromatics; importantly, time-resolved kinetics measurements on the sol-gel thin films established that the same 3R mechanism observed in solution prevails in the film. A 45-fold enhancement of the Tb^{3+} luminescence intensity is triggered when a 50 μM solution of biphenyl contacts the patterned microstructure. Equivalent concentrations of analyte added to aqueous solutions of **3** generate significantly smaller enhancements (e.g., 8-fold enhancement for [biphenyl] = 50 μM), suggesting that analyte asso-

Scheme 2

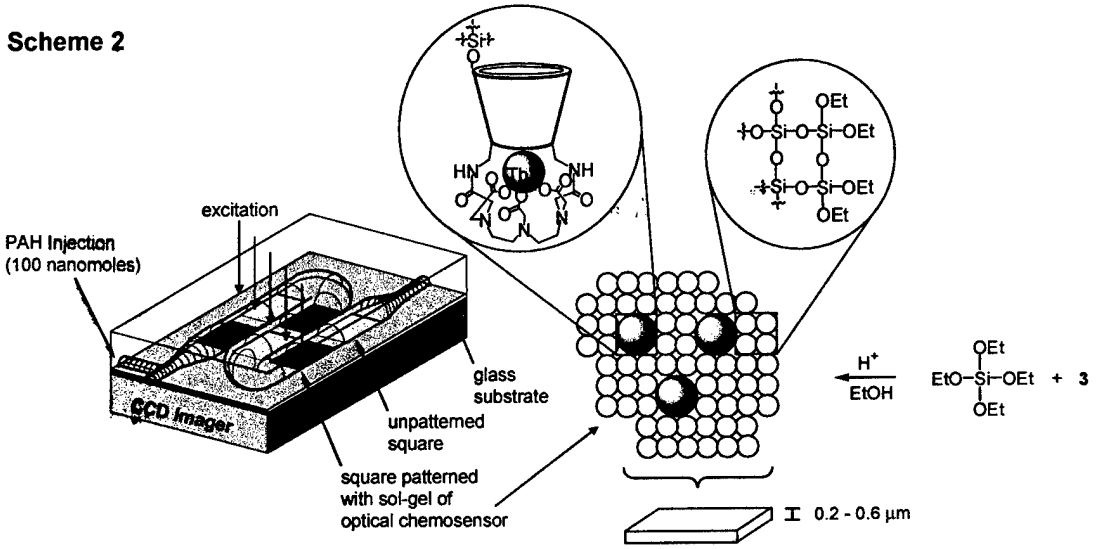

ciates more strongly to the CD bucket of **3** when immobilized in sol-gel films. The Tb^{3+}-luminescence enhancement proves to be concentration-dependent, increasing monotonically with the concentration of biphenyl; detection of biphenyl at 5 μM is easily achieved. We estimate from the extrapolation of these data to the limits of our detector response that analyte can be detected reliably to 100 nM. The μFOC platform exhibits considerable structural and optical integrity; the signal response of **3** is maintained over a period of greater than three months with little degradation of the signal response (<10% change in signal intensity).

3. Pressure and Temperature Sensing at Aerodynamic Surfaces

3.1. Quantum Dots as Temperature Probes for Pressure Sensitive Paints

Beyond the chemical environment, the Air Force faces challenges in sensing many different types of physical phenomena. The measurement of surface pressures in aerodynamics testing is especially prominent in Air Force efforts to design high performance aircraft and engines. Surface pressure measurements relying on the longstanding and conventional single-point "macroscopic" methods based on taps and transducers are being replaced with multi-point "molecular" methods based on the luminescence from pressure sensitive paints (PSPs). PSPs contain a luminescent probe that is sensitive to the concentration of oxygen in the coating; the luminescence variance arising from oxygen quenching within the paint allows for the creation of real-time optical maps of surface pressure variations on aerodynamic surfaces. A significant challenge to this technique is that the luminescence of the pressure probe is also invariably sensitive to temperature fluctuations. The temperature and pressure dependencies must be disentangled for the accurate measurement of pressure. The Air Force has initially addressed this problem by performing a separate temperature calibration run. However, owing to the significant expense of running wind tunnel facilities, the Experimental Operations and Diagnostics Branch of the Aeromechanics Division of the Flight Dynamics Directorate at Wright Patterson AFB, was interested in eliminating the temperature calibration run in its subsonic wind tunnel facility. We addressed this Air Force need by setting out to develop a luminescence "thermometer" that could be incorporated into PSPs currently used by the Air Force.

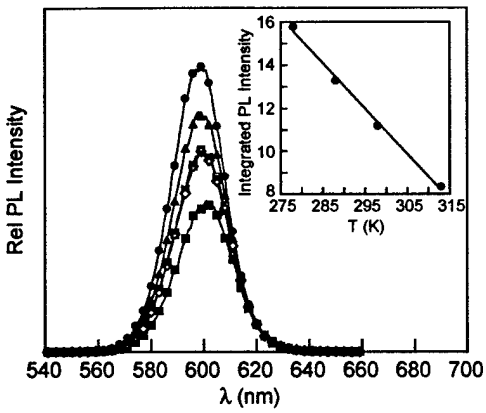

***Figure** 7. The photoluminescence emission spectra for polymer supported (CdSe)ZnS QDs excited at 480 nm at near ambient temperatures in the following order: 298 (×), 313 (■), 298 (Δ), 288 (▲), 278 (●), 298 K (◊). Inset: variation in integrated photoluminescence emission intensity with temperature and a least-squares linear regression analysis of the data.*

Our initial studies focused on using the metal-to-ligand charge transfer excited state of metal polypyridyls [*3.1.4.6, 3.1.4.7*]. But our attention soon turned to nanocrystalline CdSe particles encapsulated by a passivating layer of ZnS. This line of work was greatly facilitated by the informal collaboration between the PI and his colleague, Professor Moungi Bawendi, who leads a preeminent program in nanocrystal research. We have shown that (CdSe)ZnS quantum dots (QDs) possess extremely attractive properties for application as temperature sensitive probes (TSPs) [*3.1.4.8, 3.1.4.9*]. The emission mechanism of the QDs involves electron-hole recombination within the inorganic core of the particle, which is insensitive to collisional quenching by oxygen. Hence the temperature profile of bilumophoric coatings containing (CdSe)ZnS QDs and a pressure sensitive probe is provided directly from monitoring the luminescence of the dots. Figure 7 shows the temperature dependence of the emission band for (CdSe)ZnS QDs. Spectra were recorded at intervals throughout the temperature range of 5-40 °C. The linear change in emission intensity of 1.5% per °C throughout the entire 35 °C range far exceeded Air Force design specifications by 0.5% per °C. The exceptional photostability of the QDs and the reversibility of the luminescence change with temperature are in evidence from the almost perfect superposition of the 25 °C-emission bands of Figure 7 recorded at the beginning, middle, and end of the experiment. As expected, the QD luminescence showed absolutely no dependence on oxygen concentration.

The QDs provide additional conveniences for the design of pressure- and temperature-sensitive bilumophoric coatings. The near-Gaussian emission band of narrow widths (fwhm = 30 nm) may be produced across the full range of the visible spectrum (400 nm (15 Å nanocrystals) - 700 (100 Å nanocrystals)); accordingly the position of the emission band for luminescence thermometry can be easily tuned away from the emission band used for pressure measurements. At the same time, the QDs possess a very broad and featureless absorption profile with an extinction coefficient that is essentially invariant from 300 to 480 nm. Thus the QD emission needed for thermometry measurements may be achieved with excitation wavelengths that are coincident with excitation of the pressure-sensitive lumophore. Finally, the (CdSe)ZnS QDs were incorporated into PSP binders with the same preparative conditions used to formulate PSPs under study and use at Wright Patterson Labs.

The significant temperature dependence of the luminescence combined with its insensitivity to quenching by oxygen establishes these (CdSe)ZnS-based materials as an attractive new class of optical indicators for luminescence thermometry applications. The QD-based technology was directly passed from this AFOSR program to the Aerodynamics Configuration Branch (AFRL/VAAA) of the Air Vehicles Directorate at Wright Patterson Air Force Base for testing and evaluation. This transition was made possible by an STTR involving Innovative

Scientific Solutions, Inc. (ISSI), a sub-contractor to the Air Force. All expectations of the QDs as temperature probes were confirmed at Air Force facilities in 6.2 tests. The results of this work have been described in a recent joint publication from the PI labs, AFOSR and ISSI [*3.1.4.10*]. We hope that QD paints containing (CdSe)ZnS QDs as TSPs will be commercialized in 6.3 ventures at Arnold and Wright Patterson AFB over the next two years.

4. Development of the MTV Technique for the Micro-/Nanodomain

The quantitative measure of turbulent flows at aerodynamic boundaries is another physical sensing problem that has occupied this research program. We have invented an optical technique called Molecular Tagging Velocimetry (or MTV) [*3.1.4.11* and *3.1.4.12*], which allows us to physically sense flow by precisely describing the velocity profile of a fluid. In the MTV experiment, luminescent supramolecular tracers are dissolved in a fluid gas or liquid and a grid of laser lines is imposed upon the flow by shining a laser beam off of a grating to produce a glowing grid, defined by the luminescence from the optical supramolecule tracer. The tracer must exhibit a bright, non-quenchable luminescence, which is sufficiently long-lived to convect with the flow (μs to ms depending on the fluids problem). The deformation of the grid as it moves with the flow is recorded with a CCD camera. By measuring the distance and direction each grid intersection travels and knowing the time delay between each image, the two velocity components in the grid plane may be determined (the out-of-plane velocity can be determined with a second CCD camera). Parameters important to the fluid physicist, such as turbulence intensities, the Reynolds stress and vorticity may be calculated.

Prior to the DURIP funding period, supramolecular tracers developed in our labs enabled us to image flows to 50 ms. However, many interesting flow structures, including those on micro- and nano-dimensions, move at much slower speeds (especially near boundary walls). To advance the MTV technique to the micro-/nano-dimension, we became interested in using photoactivated dye tracers that could be *reversibly* caged and decaged.

We sought to develop dyes based on principles previously established by Mann and co-workers in their studies of $CpRu^{II}$ arene and aromatic dye complexes in nonaqueous solutions. In this design, a dye complexed to the metal head-group does not luminesce since the excited state will decay nonradiatively via the low-lying ligand field states of the metal head group. If the ligand field state is dissociative with respect to ligand, then laser excitation of the complex frees the laser dye from the metal complex. As applied to the MTV technique, once liberated from the deactivating head group, the laser dye is free to emit upon delivery of a second excitation pulse to image the dye. The luminescent dye can be tracked indefinitely by simple fluorescence imaging approaches with a second interrogating laser pulse (or other source to illuminate the flow field). The image is produced by the exciting laser pattern; a fluorescent dye is spatially produced only in regions where the laser has excited the fluid.

In our studies, we found that the Mann chemistry does not translate to aqueous solution because the $18e^-$ aquo complex, $[CpRu^{II}(H_2O)_3]^+$, produced upon dye liberation was too stable. We thus sought to labilize the coordinated waters so that the freed dye could re-attach to the metal head group, thus making the system reversible. Use of $Cp^*Ru^{II}(MeCN)_3^+$ as a starting material has proved to be convenient in the synthesis of the two caged dye complexes shown in Figure 8. Both compounds have been isolated and characterized by x-ray crystallography. Interestingly, the acridone (PSA) complex is a dimer formed from the attachment of the Cp^*Ru^{II} head group to

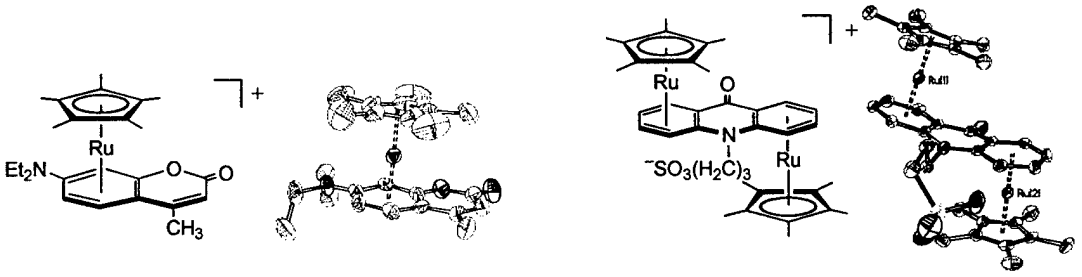

Cp*Ru(C460)$^+$ **(Cp*Ru)$_2$(PSA)$^+$**

Figure 8. *Isolation and structural characterization of new, reversible, caged dye tracers for application of the MTV technique to measure slow flows in microfluidic devices.*

opposite faces of the acridone dye. This result is obtained owing to the presence of two phenyl groups in the acridone ring system. The dimer problem is eliminated when only one phenyl group is present in the dye ring system as exemplified by the caged coumarin (C460) complex. Both complexes are stable in air and water.

The dyes, shown in Figure 8, function as reversible photocaged tracers for the MTV technique. Photolysis of both complexes, which are initially non-emissive, with 305 nm light frees the dye. This process has been confirmed by UV-vis absorption and emission spectroscopy. The luminescence of the freed dye is intense and easily imaged by the MTV technique [*manuscript in preparation*]. We are currently implementing the tracers for the measurement of flows in small channels.

3.5. List of Publications relying on DURIP Instrumentation

1. "Buckets of Light"; Christina M. Rudzinski and Daniel G. Nocera, in *Optical Sensors and Switches*; V. Ramamurthy and K. S. Schanze, K. S. (Eds.); Molecular and Supramolecular Photochemistry, vol. 7; Marcel Dekker: New York, **2001**, p. 1-91.
2. "Optimized Detection of Aromatic Hydrocarbons in Aqueous Solution by Lanthanide-Ion Modified Cyclodextrin Supramolecules"; Christina M. Rudzinski, Scott D. Carpenter and Daniel G. Nocera, submitted to *Chemistry – Eur. J.*
3. "Spectroscopic and Photophysical Properties of Hexanuclear Rhenium(III) Chalcogenide Clusters"; Thomas G. Gray, Christina M. Rudzinski, Emily E. Meyer, R. H. Holm and Daniel G. Nocera, *J. Am. Chem. Soc.* **2003**, *125*, 4755-70.
4. "Excited-State Distortion of Rhenium(III) Sulfide and Selenide Clusters"; Thomas G. Gray, Christina M. Rudzinski, Emily E. Meyer and Daniel G. Nocera, *J. Phys. Chem.* **2003**, submitted for publication.
5. "A Supramolecular Microfluidic Optical Chemosensor"; Christina M. Rudzinski, Albert M. Young and Daniel G. Nocera, *J. Am. Chem. Soc.* **2002**, *124*, 1723-7.
6. "Compounds of general interest. A luminescent complex of Re(I): fac-$[Re(CO)_3(bpy)(py)](CF_3SO_3)$ (bpy = 2,2′-bipyridine; py = pyridine). Erick J. Schutte, B. Patrick Sullivan, Christopher J. Chang and Daniel G. Nocera, Inorg. Synth. **2002**, *33*, 227-30.

7. "[Ru(4,7-diphenyl-1,10-phenanthroline)$_3$]Cl_2"; Glen W. Walker and Daniel G. Nocera, *Inorg. Synth.* **2004,** in press.

8. "Quantum dot optical temperature probes"; Glen W. Walker, Vikram C. Sundar, Christina M. Rudzinski, Moungi G. Bawendi and Daniel G. Nocera, *Appl. Phys. Lett.* **2003**, submitted for publication.

9. "Temperature-Sensing Composition"; Alfred A. Barney, Moungi G. Bawendi, Vikram C. Sundar, Daniel G. Nocera, Christina M. Rudzinski and Glen W. Walker, Application filed by MIT on 9 February 2001 (serial number 09/779,437); MIT Internal Case #8800 (2001). U.S. Pat. Appl. Publ. 2002110180, **2002.**

10. "Investigation of Advanced Luminescent Probes and Paint Architectures"; Gary A. Dale, Larry P. Goss, Neal A. Watkins, Daniel G. Nocera, *Proc. Int. Instr. Symp.* **2001**, *47*, 10-25.

11. "Molecular Tagging Velocimetry Maps Fluid Flows"; Manooch M. Koochesfahani and Daniel G. Nocera, *Laser Focus* **2001**, *37(6)*, 103-8.

12. "Molecular Tagging Velocimetry: A Review of Techniques, Chemical Concepts, and Applications"; Manoochehr M. Koochesfahani and Daniel G. Nocera, *Exp. Fluids* **2003**, to be submitted.